A General Linear Geometric Matrix for a Fully Compatible Finite Element

DAVID V. WALLERSTEIN*
Virginia Polytechnic Institute, Blacksburg, Va.

IN the solution of rectangular plate problems by the finite element method, the use of the fully compatible element of Ref. 1 is becoming more and more prevalent. The accuracy of this element for the solution of bifurcation buckling problems in plates has been demonstrated in Ref. 2.

To date most of the published literature employing this element has examined plate buckling subject to either uniform compressive in-plane loading or to constant shear loading. In-plane triangular loading or other types of linear in-plane loading is usually approximated with the use of uniform step loading as in Ref. 3. This necessitates the use of a larger number of elements in order to adequately approximate the loading condition.

If a load relationship of the form

$$N = A + Bx + Cy + Dxy \tag{1}$$

is assumed, where N represents any one of the three in-plane loading forces N_x, N_y, or N_{xy}, a nodal load relationship of the form

$$N = N_{11} + (N_{21} - N_{11})\xi + (N_{12} - N_{11})\eta + (N_{11} + N_{22} - N_{12} - N_{21})\xi\eta \tag{2}$$

results. In the preceding, the N_{ij}'s $i = 1, 2$; $j = 1, 2$, are the nodal forces and ξ, η are the nondimensionalized x, y coordinates of the plate.

Using Eq. (2) in the expression for the work of in-plane force for a plate element, the initial stress or geometric matrix takes the form:

$$\begin{aligned}\underset{16\times16}{[S]} = {} & \beta^{-1}N_{x11}[f_{x,0}] + \beta^{-1}(N_{x21} - N_{x11})[f_{x,x}] + \\ & \beta^{-1}(N_{x12} - N_{x11})[f_{x,y}] + \beta^{-1}(N_{x11} + N_{x22} - N_{x12} - N_{x21}) \times \\ & [f_{x,xy}] + 2N_{xy11}[f_{xy,0}] + 2(N_{xy21} - N_{xy11})[f_{xy,x}] + \\ & 2(N_{xy12} - N_{xy11})[f_{xy,y}] + 2(N_{xy11} + N_{xy22} - \\ & N_{xy12} - N_{xy21})[f_{xy,xy}] + \beta N_{y11}[f_{y,0}] + \\ & \beta(N_{y21} - N_{y11})[f_{y,x}] + \beta(N_{y12} - N_{y11})[f_{y,y}] + \\ & \beta(N_{y11} + N_{y22} - N_{y12} - N_{y21})[f_{y,xy}]\end{aligned} \tag{3}$$

where N_{ijk} $i = x, y, xy$, $j = 1, 2$, $k = 1, 2$ are the nodal loading components and the twelve 16×16 matrices are defined by the integral relationships

$$[f_{x,\phi}] = \int_0^1 \int_0^1 \psi \cdot \{f_b\}_\xi \lfloor f_b \rfloor_\xi \, d\xi \, d\eta$$

$$[f_{xy,\phi}] = \int_0^1 \int_0^1 \psi \cdot \{f_b\}_\xi \lfloor f_b \rfloor_\eta \, d\xi \, d\eta$$

$$[f_{y,\phi}] = \int_0^1 \int_0^1 \psi \cdot \{f_b\}_\eta \lfloor f_b \rfloor_\eta \, d\xi \, d\eta$$

and $\beta = a/b$ is the plate aspect ratio. In the preceding (ϕ, ψ) are the set of ordered pairs such that:

$$\{(\phi, \psi) \mid (0, 1), (x, \xi), (y, \eta), (xy, \xi\eta)\}$$

and $[f_b]$ is the 1×16 row matrix representing the nondimensional coefficients in the displacement relationship

$$W(\xi, \eta) = \sum_{i=0}^{3} \sum_{j=0}^{3} A_{ij} \xi^i \eta^j = \lfloor f_b \rfloor \{W_n\}$$

$\{W_n\}$ is the 16×1 column matrix representing the nodal displacements. Typical terms are

$$\{W_n\} = \lfloor W_{11}, aW_{\xi 11}, bW_{\eta 11}, abW_{\xi\eta 11}, \ldots \rfloor^T$$

The subscripts ξ, η of $\{f_b\}$ and $[f_b]$ and W_{11} indicate that partial differentiation with respect to the particular subscript has been performed.

These integrals can readily be evaluated with the aid of programing systems such as the Formac Interpreter Programming System. The resulting 16×16 matrices can be stored as permanent block data with no storage sacrifice. The algorithms necessary to program the geometric matrix are easy to construct.

The terms of Eq. (3) resulting in uniform compressive loading in the x and y directions are those terms containing $[f_{x,0}]$ and $[f_{y,0}]$, respectively. The term containing $[f_{xy,0}]$ represents the effect of constant shear loading. The remaining terms represent the effects of linear loading conditions as simultaneous functions of both in-plane loading coordinates. These additional terms greatly facilitate the solution of stability problems in plates under complex loading states.

The results of Table 1 demonstrate the accuracy of the element of Ref. 1 under the influence of some simple linear varying loads. From the table, two observations should be made. First, the mesh size and the number of half waves, into which the plate buckles, are interrelated. Second, a relatively coarse mesh yields results well within the confines of engineering accuracy. The most striking example of this is the square simply supported plate under a triangular in-plane load distribution with a 2×2 mesh.

It should be mentioned that the eigenvalues of Table 1 were determined by an inverse power method with a shift.[6] The method utilizes the Choleski procedure of matrix decomposition which has been specialized for banded matrices.

Table 1 Buckling coefficients of simply supported and clamped isotropic plates subjected to linearly varying uniaxial and biaxial compression (see note 3)

Loading and Boundary Conditions (2)	Mesh m x n	K	K (Known)	% Difference	Reference for known data
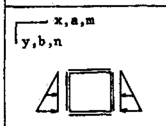	2x2	7.8712	7.8	0.91	4
	3x6	7.8153		0.20	
	4x4	7.8151		0.19	
	4x8	7.8131		0.17	
	6x3	7.8192		0.25	
	6x6	7.8126		0.16	
	8x4	7.8142		0.18	
	8x8	7.8122		0.15	
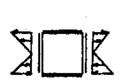	3x6	25.7584	25.528	0.90	5(1)
	4x6	25.6196		0.36	
	4x8	25.6085		0.32	
	6x3	25.9312		1.58	
	8x4	25.6288		0.39	
	8x8	25.5386		0.04	
	12x6	25.5454		0.07	
	12x8	25.5343		0.02	
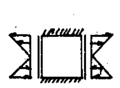	3x6	40.0588	39.7	0.90	4
	4x4	40.5153		2.07	
	4x6	39.9120		0.53	
	4x8	39.8084		0.27	
	6x3	42.5111		7.08	
	6x6	39.8438		0.37	
	8x8	39.7275		0.07	
	10x10	39.6950		0.01	
	12x8	39.7225		0.07	
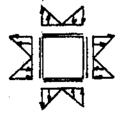	4x4	13.3650	---	---	
	6x6	13.3053			
	8x8	13.2957			
	10x10	13.2929			

Notes: 1. Determined with seventh approximation.
2. $a/b = 1$; $\nu = 1/3$ clamped simple
3. Results of this table were taken from Reference 7.

References

[1] Bogner, F. K., Fox, R. L., and Schmit, L. A., Jr., "The Generation of Inter-Element Compatible Stiffness and Mass Matrices by the Use of Interpolation Formulas," *Conference on Matrix Methods in Structural Mechanics*, AFFDL-TR-66-80, 1966, Air Force Flight Dynamics Lab., Wright-Patterson Air Force Base, Ohio, pp. 397–443.

[2] Garson, W. G. and Newton, R. E., "Plate Buckling Analysis Using a Fully Compatible Finite Element," *AIAA Journal*, Vol. 7, No. 3, March 1969, pp. 527–529.

Received October 22, 1971.

* Assistant Professor of Minerals Engineering; formerly Design Specialist, Lockheed-California Company, Burbank, Calif.

[3] Isakson, G., Armen, H., Jr., and Pifko, A., "Discrete-Element Methods for the Plastic Analysis of Structures," CR-803, 1967, NASA.

[4] Bleich, F., *Buckling Strength of Metal Structures*, McGraw-Hill, New York, 1952.

[5] Timoshenko, S. P. and Gere, J. M., *Theory of Elastic Stability*, McGraw-Hill, New York, 1961.

[6] Contini, R., "Procedures for the Determination of Eigenvalues of Systems of Linear Algebraic Equations Involving Banded Matrices," Rept. 24102, 1971, Lockheed-California Co.

[7] Hubka, R. E. and Wallerstein, D. V., "A Displacement-Type Finite Element Analysis of Bifurcation Buckling of Rectangular Elastic Plates Based on a Conforming Rectangular Element," Rept. 23841, July 1970, Lockheed-California Co., Burbank, Calif.

General Response of Resistance Thermometers and Thermocouples in Gases at Low Pressures

M. R. Davis*

The University of New South Wales, Kensington, N.S.W., Australia

ALL types of thermometer used to measure gas temperature rely upon the thermal contact between the sensing element and the gas to achieve a good reponse. It is necessary that this thermal contact should predominate over the thermal contact between the element and its mountings if the sensor is not to indicate the temperature of the mountings. At low-gas pressures, the surface heat-transfer coefficient between the sensing element and the gas can be sufficiently small so that the sensor tends to adopt the temperature of the mountings rather than that of the gas. Heat-transfer coefficients from fine wires under these conditions have recently been discussed by Rajasooria and Brundrin.[1] In this Note, the general response of resistance wires and wire thermocouple junctions is considered in terms of the relation between the average wire temperature (T_{av}) (or junction temperature (T_c) for the thermocouple) and the temperature of the gas (T_f) and wire mountings (T_o). It is assumed that the mountings are sufficiently massive so that their temperature is not affected by the flow.

The thermal equilibrium of an unheated resistance wire is determined by the equation for heat conduction along the wire length (direction x), the local wire temperature (T) being given by

$$d^2T/dx^2 - (4h/kd)(T - T_f) = 0 \tag{1}$$

where h is the heat-transfer coefficient for the surface of the wire, of diameter d and thermal conductivity k. These parameters are assumed constant over the wire length. The equation is identical to that used by King[2] and many others subsequently, except that the heating term due to the current in the wire is omitted in this case. The solution to this equation is determined by the boundary conditions ($T = T_0$ at $x = \pm l$) and is given by

$$\theta = (T - T_o)/(T_f - T_o) = 1 - \cosh(a\eta)/\cosh(al) \tag{2}$$

where $a = (4h/kd)^{1/2}$ and $\eta = x/l$. The average wire temperature, obtained simply by integrating over the wire length ($-l < x < l$), is

$$\theta_{av} = (T_{av} - T_o)/(T_f - T_o) = 1 - \sinh(al)/[al\cosh(al)] \tag{3}$$

Figure 1 shows a set of dimensionless temperature profiles along the wire, the average temperature increasing and the profile becoming flatter as al becomes large and the wire temperature approaches the fluid temperature. Figure 2 shows the variation of average wire temperature, this being midway between support and fluid temperatures (i.e., $\theta_{av} = 0.5$) if $al = 1.94$.

For some typical resistance wires (Table 1) it may be seen that

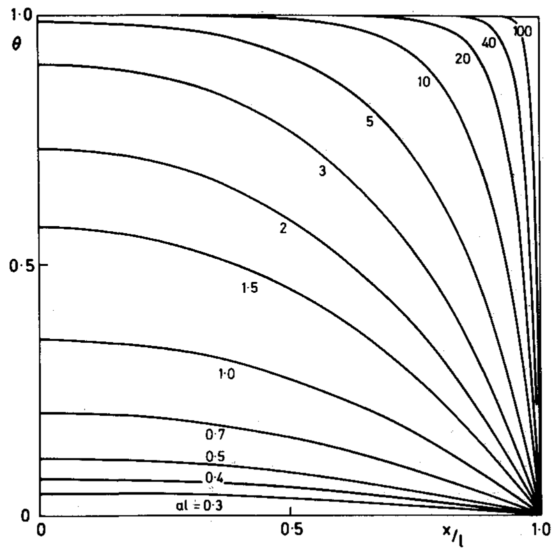

Fig. 1 Temperature distributions along resistance wires.

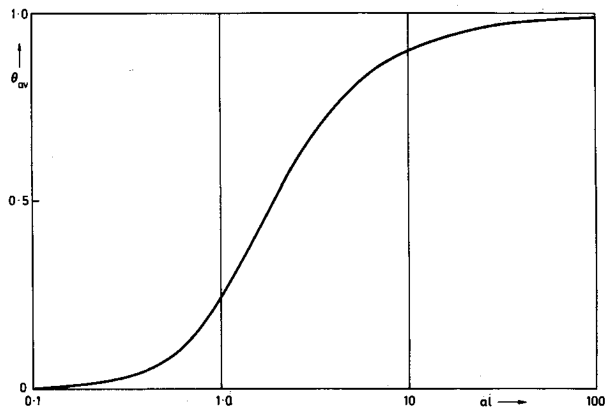

Fig. 2 Variation of average resistance wire temperature.

the heat transfer coefficient corresponding to a relatively low response to fluid temperature (e.g., $\theta_{av} = 0.1$) lies in the range of free molecular heat transfer at the wire surface. The heat transfer coefficient in a static gas is then given by (Kennard[3])

$$h = (C_v + R/2)\alpha p/(2\pi MRT_f)^{1/2} \tag{4}$$

where α is the surface thermal accommodation coefficient, M, C_v and R being the molecular weight, specific heat at constant volume and gas constant for the gas. Using this equation with $\alpha = 1$, values of the air pressure corresponding to $\theta_{av} = 0.1$ are also shown in Table 1. When the gas is moving at a significant Mach number, the analysis of Oppenheim[4] or Schaaf[5] may be used to determine the surface heat-transfer coefficient under free molecular conditions. For the limiting conditions of large M (approximately $M > 2$) the Stanton number becomes constant and the heat transfer coefficient is determined directly by the gas flux density. Flux density values corresponding to $\theta_{av} = 0.1$ are also shown in Table 1 for the typical wires considered.

Where a thermocouple is constructed of a bead junction supported by the two connecting wires, a similar analysis may be applied by using Eq. (1) for each support wire (with $T = T_o$ at $x = -l_1$ and $x = +l_2$). Constants $a_1 = (4h_1/k_1d_1)^{1/2}$ and $a_2 = (4h_2/k_2d_2)^{1/2}$ are introduced for each support wire and the equation for bead thermal equilibrium is also required to solve for the junction bead temperature T_c. That is, assuming the same heat-transfer coefficient h for all surfaces.

$$hA(T_c - T_f) = (\pi d_2^{\,2}k_2/4)(dT_2/dx)_{x=0} - (\pi d_1^{\,2}k_1/4)(dT_1/dx)_{x=0} \tag{5}$$

where A = area of bead surface at $x = 0$. This leads, together

Received October 26, 1971.

* Lecturer, Department of Fluid Mechanics and Thermodynamics, School of Mechanical and Industrial Engineering.